

Published in final edited form as:

J Cardiovasc Pharmacol. 2010 July ; 56(1): 80–90. doi:10.1097/FJC.0b013e3181e0bc6b.

AZD1305 Exerts Atrial-Predominant Electrophysiological Actions and Is Effective in Suppressing Atrial Fibrillation and Preventing Its Re-induction in the Dog

Alexander Burashnikov, PhD, Andrew C. Zygmunt, PhD, Jose M. Di Diego, MD, Gunilla Linhardt, MSc*, Leif Carlsson, PhD*, and Charles Antzelevitch, PhD

Masonic Medical Research Laboratory, Utica, NY

*AstraZeneca R&D Mölndal, Sweden

Abstract

Recent development of drugs for the treatment of atrial fibrillation (AF) has focused on atrial-selective agents. We examined the atrioventricular differences in sodium channel block of the antiarrhythmic agent AZD1305 in atria and ventricles of anesthetized dogs *in vivo*, in canine isolated arterially-perfused preparations *in vitro* and in isolated myocytes using whole-cell patch-clamp techniques. AZD1305 did not change heart rate or blood pressure *in vivo* but prolonged action potential duration and increased effective refractory period, diastolic threshold of excitation, and conduction time preferentially in atria both *in vitro* and *in vivo*. AZD1305 reduced the maximum rate of rise of the action potential (AP) upstroke (V_{\max}) predominantly in atria ($-51 \pm 10\%$ in atria vs. $-31 \pm 23\%$ in ventricles; $3 \mu\text{M}$; cycle length = 500 ms). Fast sodium current (I_{Na}) was blocked by AZD1305 to a greater degree in atrial vs. ventricular myocytes (particularly tonic inhibition). In coronary-perfused right atria, AZD1305 very effectively prevented induction of persistent acetylcholine-mediated AF and, in a different set of atria, terminated persistent AF (in 5/5 and 7/8 atria, respectively). In conclusion, AZD1305 exerts atrial-predominant sodium channel-blocking effects *in vitro* and *in vivo*, and effectively suppresses AF.

Keywords

Pharmacology; electrophysiology; sodium channel blocker; potassium channel blocker; arrhythmia

INTRODUCTION

An important limitation of currently available antiarrhythmic agents (AAD) available for the treatment of atrial fibrillation (AF) is a risk for induction of severe ventricular proarrhythmias. Atrial-selective AADs are being developed to eliminate or reduce the risk of inducing ventricular proarrhythmia. Selective prolongation of the atrial effective refractory period (ERP) can be achieved through specific block of ion channels such as I_{Kur} , I_{Na} or I_{KACH} .^{1–5} Most atrial-selective investigational drugs block multiple ion channels at concentrations that are effective in suppressing AF (e.g., vernakalant and AZD7009 blocks I_{Na} , I_{Kr} and I_{Kur} , AVE0118

Copyright © Lippincott Williams & Wilkins.

Address for correspondence: Dr. Charles Antzelevitch PhD Masonic Medical Research Laboratory 2150 Bleecker Street, Utica, N.Y. 13501 FAX: (315)735-5648 ca@mmrl.edu.

Conflict of Interest Disclosure: Dr. Leif Carlsson and Gunilla Linhardt are employees of AstraZeneca R&D. Dr. Charles Antzelevitch received a grant from AstraZeneca R&D.

inhibits I_{Kur} , I_{to} , I_{Kr} , and I_{Na} , ranolazine blocks I_{Na} and I_{Kr}).^{3; 6-9} AZD1305 is an investigational AAD, structurally related to AZD7009,¹⁰ which was shown to be highly effective for acute termination of AF in both experimental and clinical settings.¹¹⁻¹⁴ In addition to its atrial-selective ERP prolongation, AZD7009 was shown to exert atrial-predominant depression of sodium channel-mediated parameters (diastolic threshold of excitation and conduction velocity),^{11; 15} suggesting that it is an atrial-selective sodium channel blocker. The present study was undertaken to compare the electrophysiological effects of AZD1305 in canine atria and ventricles *in vitro* and *in vivo* as well as in isolated atrial and ventricular myocytes. In addition, the anti-AF efficacy of AZD1305 was evaluated in an experimental model of AF *in vitro*.

METHODS

This investigation conforms to the Guide for Care and Use of Laboratory Animals published by the National Institutes of Health (NIH publication No 85-23, Revised 1996) and was approved by the Animal Care and Use Committee of the Masonic Medical Research Laboratory.

In vitro studies

Dogs (n=63) weighing 20-25 kg were anticoagulated with heparin (200 IU/kg) and anesthetized with pentobarbital sodium (35 mg/kg, i.v.). The chest was opened via a left thoracotomy, the heart excised, placed in a cardioplegic solution consisting of cold (4°C) Tyrode's solution containing 8.5 mM $[K^+]_o$ and transported to a dissection tray.

Arterially-perfused canine right atrium

Three-fourths of both ventricles were quickly removed. The ostium of the right coronary artery was cannulated with polyethylene tubing (i.d., 1.75 mm; o.d., 2.1 mm) and the preparation was perfused with cold Tyrode's solution (12 to 15°C) containing 8.5 mM $[K^+]_o$. With continuous coronary perfusion, all ventricular branches of the right coronary artery were immediately clamped with metal clips. The entire right atrium (RA) with a thin rim (<1 cm) of right ventricular tissue was carefully dissected from the remaining tissues and then the preparation was unfolded. Ventricular right coronary branches as well as the cut atrial branches were ligated using silk thread. The preparation was placed in a temperature-controlled bath (8 × 6 × 3 cm) and perfused at a rate of 8 to 10 mL/min with Tyrode's solution (37.0±0.5°C).

Arterially-perfused canine left ventricular wedge

Transmural wedges with dimensions of approximately 3 × 1.5 × 1.5 cm were dissected from the left ventricle (LV). The tissues were cannulated via a small (diameter ~150 µm) coronary artery and perfused with cardioplegic solution. The preparations were then placed in a small tissue bath and arterially-perfused with Tyrode's solution (37.0±0.5°C).

For both atrial and ventricular preparations, the composition of the Tyrode's solution was (in mM): NaCl 129, KCl 4, NaH₂PO₄ 0.9, NaHCO₃ 20, CaCl₂ 1.8, MgSO₄ 0.5, and D-glucose 5.5, buffered with 95% O₂ and 5% CO₂. The solution was delivered to the artery by a roller pump (Cole Parmer Instrument Co., Niles, IL, USA).

Electrophysiological assessments

Transmembrane action potential (AP) recordings were obtained using floating glass microelectrodes (2.7 M KCl, 10 to 25 MΩ DC resistance) connected to a high input impedance amplification system (World Precision Instruments, Sarasota, FL, USA). The signals were displayed on oscilloscopes, amplified, digitized and analyzed (Spike 2, Cambridge Electronic

Design, Cambridge, England). An electrocardiogram (pseudo-ECG) was recorded using two electrodes consisting of AgCl half cells attached to Tyrode's-filled tapered polyethylene electrodes which were placed in the bath solution 1.0 to 1.2 cm from the opposite ends of the atrial and ventricular preparations. The diastolic threshold of excitation (DTE) was determined by increasing stimulus intensity in 0.01 mA steps. The ERP was measured by delivering premature stimuli after every 10th regular beat at a pacing cycle length (CL) of 500 ms (with 5 to 10 ms resolution; stimulation with a $2 \times$ DTE amplitude). Post-repolarization refractoriness (PRR) was defined as the difference between ERP and action potential duration at 75% repolarization (APD₇₅) in atria and action potential duration at 90% repolarization (APD₉₀) in ventricles (ERP corresponds to around APD₇₅ in atria and APD₉₀ in ventricles, respectively).³ Maximum rate of rise of the AP upstroke (V_{\max}): Stable action potential recordings and V_{\max} measurements are difficult to obtain in vigorously contracting perfused preparations. A large variability in V_{\max} measurements is normally encountered at any given condition, primarily due to variability in the amplitude of phase 0 of the action potential which strongly determines V_{\max} values. The effects of AZD1305 on V_{\max} were determined in coronary-perfused atria and ventricles by comparing the largest V_{\max} recorded under any given condition/region. Due to a substantial inter-preparation variability, V_{\max} values were normalized for each experiment and then averaged. Changes in conduction time were approximated by measuring the duration of the "P wave" complex in atria and the "QRS" complex in ventricles on the ECG at a level representing 10% of "P wave" or "QRS" amplitude.

Experimental protocols—Coronary-perfused atrial and ventricular preparations were equilibrated in the tissue bath until electrically stable, usually 30–60 min. The preparations were paced at a CL of 500 ms, using a pair of thin silver electrodes insulated except at their tips (bipolar rectangular pulses of 2 ms duration and twice DTE intensity). Action potentials were recorded under baseline conditions and after the addition of 1 or 3 μ M of AZD1305 to the perfusate. At least 15 min were allowed for each concentration of AZD1305 to act before the start of data collection.

The antiarrhythmic efficacy of AZD1305 was tested in an acetylcholine (ACh)-mediated model of persistent AF. Persistent AF develops in 100% atrial preparations pretreated with ACh following burst pacing or introduction of a single extrastimuli. Two separate sets of experiments were performed. In the first set, ACh was added to the solution containing 3 μ M AZD1305 (after completing the measurement of the electrophysiological effects of AZD1305) and stimulation applied in an attempt to induce AF. In the second set, persistent AF was induced first (in the presence of ACh, 1.0 μ M) and then, on the 4–6th min of on-going AF AZD1305 was added (1.0 or 3.0 μ M) to the perfusate in the continued presence of ACh. If the lower concentration of AZD1305 did not terminate AF within 20 min, the concentration was increased to 3.0 μ M. If AF was terminated, re-induction of the arrhythmia was attempted.

Isolated cardiomyocytes

Cell dissociation—Dogs of either sex were anticoagulated and anesthetized as described above, and their hearts quickly removed and placed in cold cardioplegic solution containing 12 mM KCl. A wedge-shaped section of the ventricular free wall supplied by the left anterior descending artery was perfused at a constant rate of 12 mL/min with nominally Ca-free Krebs solution for 5 min followed by nominally Ca-free Krebs solution containing type II collagenase (0.5 mg/mL, Worthington Biochemicals, Freehold, NJ, USA) and 0.1% bovine serum albumin for 12 to 20 min. Right atrial myocytes were obtained from an unfolded right atrial preparation with a rim of the right ventricle cannulated and perfused through the ostium of the right coronary artery. The perfusion solutions were warmed to 37°C and saturated with a gas mixture of 95% O₂/5% CO₂. After perfusion, 1- to 2-mm thick shavings of tissue were dissected from the epicardial and endocardial regions. Minced tissues from each region were incubated in

fresh Krebs solution containing 0.3 mM CaCl_2 , 3% albumin, and collagenase (0.5 mg/mL). Myocytes were harvested at 15-min intervals, centrifuged at 200-300 rpm for 2 min, resuspended in Tyrode's solution containing 0.5 mM CaCl_2 , and stored at room temperature. The composition of Krebs solution used for dissociation of cells contained (in mM): 118.5 NaCl, 12 KCl, 14.5 NaHCO_3 , 1.2 KH_2PO_4 , 1.2 MgSO_4 , and 11.1 glucose, pH was 7.4. The Tyrode's solution contained (in mM) 135 NaCl, 5.4 KCl, 1.0 MgCl_2 , 0.5 or 2.0 CaCl_2 , 10 glucose, 0.33 NaH_2PO_4 , and 10 N-2-hydroxyethylpiperazine-N'-2-ethanesulfonic acid (HEPES); pH was adjusted to 7.4 with NaOH.

Voltage clamp solutions—Fast I_{Na} was measured using both ruptured patch voltage clamp at 15°C in reduced sodium solutions, and as the lidocaine-sensitive cell-attached macro current at 37°C in full sodium. External solution used in the ruptured patch voltage clamp experiments contained (in mM): 2 CaCl_2 , 10 glucose, 1 MgCl_2 , 40 NaCl, 120 N-methyl-D-glucamine, 10 HEPES, pH was adjusted to 7.4 with HCl. CdCl_2 (300 μM) was added to this external solution to block the L-type Ca current and to partially reduce I_{Na} . Tartaric acid (10 μM) was added to the control solution such that drug solutions and control solutions contained equal amounts of this vehicle. Pipette solution used in the ruptured patch voltage clamp experiments contained (in mM): 1 MgCl_2 , 5 NaCl, 145 Cs-aspartate, 10 HEPES, 5 EGTA, 5 MgATP, and pH was adjusted to 7.1 with CsOH. Pipette solution used in cell-attached patch voltage clamp experiments contained (in mM): 2 CaCl_2 , 10 glucose, 1 MgCl_2 , 4 KCl, 145 NaCl, 10 HEPES, pH adjusted to 7.4 with HCl. Normal intracellular ionic composition was undisturbed using this technique, as there was no exchange of the pipette solution with intracellular ions.

Ruptured patch voltage clamp protocols—The specific voltage clamp protocols are described in the Results section. Standard protocols were used to measure inactivation and recovery of sodium channels in the absence of AZD1305 in both left ventricular endocardial myocytes and right atrial myocytes. AZD1305 interactions with resting and inactivated states of sodium channels were assessed during trains of 60-ms pulses to -30 mV. Trains of 40 pulses were elicited over a range of holding potentials in the absence and presence of AZD1305 to yield tonic and use-dependent block. The effects of independently changing test pulse duration and the diastolic interval were used to judge the relative contributions of drug interactions with inactivated and resting states. Tonic block was measured as the decrease of I_{Na} in the presence of drug during the first pulse of the train. To evaluate development of use-dependent block, currents recorded in presence of drug were normalized to the fast inward current recorded during the first pulse. Normalized currents were plotted as a function of pulse number.

Cell-attached patch voltage clamp—Macroscopic fast I_{Na} was recorded at 37°C using cell-attached patch voltage clamp technique. In the cell-attached configuration of voltage clamp, the membrane potential is equal to the normal resting potential minus the command voltage produced by the amplifier. We have assumed resting membrane potential to be -88 mV in left ventricular endocardial cells and -83 mV in right atrial cells from normal dogs. Cell-attached recording of macro sodium currents both preserves intracellular ionic composition and allows voltage control in normal external sodium at physiological temperature. Voltage clamp command pulses were filtered at 50 kHz to slow the rate voltage change and reduce the capacitive spike during a step change in voltage. Steady state inactivation was determined using a standard double-pulse protocol with a 2 s conditioning pulse that was varied over a voltage range from -128 mV to -23 mV before and after addition of 1 mM lidocaine. I_{Na} expressed as the lidocaine-sensitive current was normalized to the current after a -128 mV conditioning pulse in ventricular myocytes and -123 mV pulse in atrial myocytes. Results were plotted as a function of conditioning pulse voltage and fit to a Boltzmann equation of the form: $y=1/(1 + \exp((x-x_0)/dx))$; where: x_0 =half-inactivation voltage, and dx =slope.

In vivo studies

Animal preparation and electrophysiological measurements—Eight Beagle dogs were anesthetized with sodium pentobarbital (30 mg/kg as an i.v. bolus, followed by a maintenance infusion of 4 to 5 mg/kg/h). The dogs were intubated and ventilated at a respiratory rate of 15 cycles/min. Before and during the experiment, the blood gases and pH in arterial blood were measured by a blood gas analyzer (ABL800 Flex, Radiometer, Copenhagen, Denmark) and, if necessary, adjusted to fall within normal physiological ranges for dogs by regulating the tidal volume and by infusing sodium bicarbonate. Ringer solution was continuously given to replace fluid loss. The rectal temperature was kept between 37.7 and 39.2°C by covering the animals and by external heating.

A percutaneous polyethylene tube to be used for administration of anesthetics, sodium bicarbonate and Ringer solution, respectively, was inserted into a brachial vein on the right leg. A second percutaneous polyethylene catheter was inserted into a brachial vein on the left leg and was used for infusion of AZD1305. A polyethylene catheter (Intramedic PE-200 Clay Adams, Becton Dickinson, Sparks, MD, USA) was inserted into the left femoral artery and advanced to the level of the aortic arch for blood pressure recording (by means of a pressure transducer, Peter von Berg Medizintechnik GmbH, Kirchseeon/Englharting, Germany) and for blood sampling.

For recording of right atrial and ventricular electrograms and for atrial and ventricular pacing, two 6F quadripolar electrophysiological recording catheters (Electrophysiology catheter-Deflectable tip, Biosense Webster Inc, Johnson & Johnson, Diamond Bar, CA, USA) were advanced into the right femoral vein and positioned high up in the right atrium (HRA) and into the right jugular vein for positioning in the apex of the right ventricle (RVE). All electrodes were advanced via introducers (6F and 7F Fast-Cath haemostasis introducer, St. Jude Medical, DAIG Division, Inc. Minnetonka, MN, USA) by means of the Seldinger Technique and correctly positioned through fluoroscopic guidance.

The ERP in the right atrium (AERP) and ventricle (VERP) was determined at a stimulation current strength approximately 20% above the threshold for pacing the atria and the ventricle, respectively. A custom-made PC-based (AstraZeneca R&D, Mölndal, Sweden) programmable stimulator and constant current pulse generator (WPI Stimulus Isolator, World Precision Instruments, Sarasota, FL, USA) were used for stimulation at a basic cycle lengths of 275 ms or 400 ms (S1). A premature extrastimulus (S2) was introduced after every 10th paced basic beat with increments of 2 ms until capture. The ERP was defined as the longest S1-S2 interval at which S2 failed to capture.

For analysis of conduction times, a His bundle electrogram was recorded by a quadripolar His-electrode catheter (6F, Electrophysiology catheter-Deflectable tip, Biosense Webster Inc, Johnson & Johnson, Diamond Bar, CA, USA) inserted through the left femoral vein and positioned across the tricuspid valve. The intraatrial conduction time was defined as the interval from start of the atrial deflection in the HRA electrogram to the start of the atrial deflection in the His bundle electrogram and the intraventricular conduction time as the width of the ventricular deflection as seen in the His bundle electrogram, respectively.

Right atrial and ventricular monophasic action potentials (MAP) were recorded by means of two 7F electrophysiological MAP-catheters (MAPCath, Deflectable Blue Curve, Biotronic GmbH & Co, Berlin, Germany) placed in right atria and ventricle, via the right and left femoral vein. The MAP electrodes were replaced for every new recording to get sufficient amplitude. The ERP were measured in the same site as the MAP recording to compare the repolarization time and the refractory time for each recording occasion, for subsequent analysis of PRR.

By means of in house custom-made amplifiers and a personal computer the body temperature, the haemodynamic variables and the electrograms were recorded at a frequency of 200 to 1000 Hz at predetermined intervals.

Experimental protocol—Approximately one hour after the completion of the preparation, pre-drug measurements commenced. After two control measurements, two doses of AZD1305 were sequentially infused according to a bolus and maintenance infusion regimen (10+50 min/dose) to reach a target pseudo steady-state plasma concentration of approximately 1 and 3 $\mu\text{mol/L}$, respectively. These plasma concentrations approximate the range of concentrations (0.5 to 2.5 μM) explored for antiarrhythmic efficacy in a recently completed dose-ranging study in AF patients. The different measurements were carried out once during each dose infusion, Blood samples for determination of plasma levels of AZD1305 were drawn 3 times per dose infusion, after the bolus infusion and exactly before and after the measurements during the maintenance infusion. The blood samples were subsequently centrifuged and the plasma stored at -20°C until analysis. The plasma concentration of AZD1305 was determined by solid phase extraction followed by liquid chromatography with tandem mass spectrometric detection according to validated methods. The lower limit of quantification was 0.015 $\mu\text{mol/L}$.

Drugs

AZD1305 (dissolved in 10 mM tartaric acid) and ACh (dissolved in distilled water) were prepared fresh as a stock of 10 mM before each experiment.

Statistics

Statistical analysis was performed using paired or unpaired Student's t test and one way repeated measures or multiple comparison analysis of variance (ANOVA) followed by Bonferroni's test, as appropriate. All data are expressed as mean \pm SD. Statistical significance was assumed at $p<0.05$.

RESULTS

Electrophysiological effects of AZD1305 in isolated coronary-perfused preparations

AZD1305 prolonged APD_{90} and ERP more in atrial than ventricular preparations (Figure 1). In atria, APD_{90} was prolonged by 3.0 μM of AZD1305 from 224 ± 12 to 298 ± 30 ms in crista terminalis and from 205 ± 8 to 283 ± 17 ms in pectinate muscle (both $p<0.001$; $\text{CL}=500$ ms; $n=12$). In the ventricles, 3.0 μM of AZD1305 prolonged APD_{90} from 167 ± 14 to 209 ± 14 ms in the M cell region and from 148 ± 12 to 191 ± 24 ms in the epicardial region (both $p<0.01$; $n=8$). While the increase of ERP in the ventricles was largely due to the increase in APD_{90} , the lengthening of ERP in the atria was due to both APD prolongation and the appearance of a pronounced PRR (Figure 1). The magnitude of phase 1 of the atrial action potential, normalized to the amplitude of phase 0, was reduced by 3 μM AZD1305 from $37\pm6\%$ to $26\pm6\%$ ($p<0.05$, $n=5$, crista terminalis, $\text{CL}=500$ ms).

AZD1305 reduced V_{max} in a rate-dependent manner in both atrial and ventricular preparations, but this reduction was much more pronounced in atria (Figure 2). The greater prolongation of action potential duration (APD) in the atrium likely contributes to the atrial-selective effect of AZD1305 to reduced V_{max} , particularly at rapid activation rates, because of elimination of the diastolic interval in atria, but not ventricles (Figure 2). The duration of the "P wave" in the atrial preparations was prolonged by AZD1305 to a much greater degree than the duration of the "QRS complex" in the ventricular wedge preparations (Figure 3A), pointing to a greater slowing of conduction velocity in atrial vs. ventricular preparations. AZD1305 significantly increased DTE in both atrial and ventricular preparations, but much more in the former (Figure 3B).

Electrophysiological and hemodynamic effects of AZD1305 in dogs in vivo

The aim of the present *in vivo* study was to assess the effects of AZD1305 at two different pseudo steady-state plasma concentrations. During infusion of the lower dose of AZD1305, plasma concentrations immediately before and after recordings of the electrophysiological and hemodynamic variables were 1.0 ± 0.08 and 1.2 ± 0.09 μM , respectively. At the higher dose level the corresponding plasma concentrations were 3.1 ± 0.25 and 4.4 ± 0.43 μM , respectively.

The infusion of AZD1305 was not associated with any effects on mean arterial blood pressure or heart rate. To examine the effect of AZD1305 on atrial and ventricular repolarization and to assess any potential effect on PRR in the right atrium and right ventricle, MAPs and ERPs measured at the MAP recording site were recorded. The results are presented in Figure 4. AZD1305 concentration-dependently and statistically significantly increased the atrial and ventricular MAP duration (panel A) at both CLs as well as the atrial and ventricular ERPs (at CL 275 ms, panel B). Quantitatively, however, the changes were more pronounced in the atrium than in the ventricle. Furthermore, when comparing the increases in the MAP duration and the ERP, it is evident that a more pronounced PRR was seen in the atrium as compared to the ventricle.

AZD1305 was found to concentration-dependently increase intraatrial conduction time to a similar extent at both CLs (Figure 5A). Although the intraventricular conduction time tended to increase the change did not reach statistical significance. Furthermore, the study also revealed a more pronounced depression of excitability in atrial vs. ventricular tissue as can be seen from the changes in DTE (Figure 5B).

Effects of AZD1305 in isolated atrial and ventricular myocytes

We have previously reported a more negative half-inactivation voltage ($V_{0.5}$) for canine right atrial myocytes when compared to left ventricular myocytes using the ruptured-patch voltage clamp technique.³ Because ruptured-patch voltage clamp causes a time-dependent leftward shift of the steady state inactivation curves that might contribute to this difference, we have performed cell-attached voltage clamp experiments in intact myocytes from normal adult dogs. Macroscopic fast I_{Na} was recorded at 37°C in 145 mM external sodium. I_{Na} was first recorded in control solution and protocols were then repeated after complete block of sodium channels by 1 mM lidocaine. Lidocaine-sensitive difference currents were plotted as a function of conditioning pulse voltage. Figure 6 confirms the presence of a more negative $V_{0.5}$ for steady-state inactivation of sodium channels (-69.6 ± 1.3 vs. -56.5 ± 0.7 mV) in canine atrial vs. ventricular myocytes when recording from intact cells in the cell-attached mode.

This difference in steady state inactivation of atrial vs. ventricular sodium channels contributes to slower recovery of atrial I_{Na} following rapid pacing at a holding potential of -90 mV. Recovery of I_{Na} following trains with diastolic intervals of 50 ms were fit to double exponentials, as shown in Figure 7. Fast time constants were 90 ± 7 ms in atrial myocytes and 101 ± 16 ms in ventricular myocytes (NS, $p > 0.05$). Atrial recovery was prolonged because of a significantly greater slow τ in atrial myocytes, 2010 ± 172 ms vs 370 ± 201 ms in atrial vs ventricular myocytes, respectively ($p < 0.05$). Ratios of the amplitudes of the fast to slow components were 2.787 and 8.583 in atrial and ventricular myocytes, respectively.

We investigated whether these differences in recovery and steady state inactivation of sodium channels might result in atrial selectivity of AZD1305 depression of I_{Na} in isolated myocytes. Interactions with resting and open states were investigated by reducing the diastolic interval (inter-pulse interval) during trains of fixed 200 ms test pulses. In the presence of 5 μM AZD1305 steady-state block increased as diastolic interval was reduced (Figure 8, lower panels). Ventricular (right panels) and atrial (left panels) steady-state sodium currents were

reduced to similar degrees ($p>0.05$) at this pulse duration. Normalized ventricular steady-state currents during the 40th pulse were 0.95 ± 0.029 , 0.89 ± 0.029 , 0.72 ± 0.078 , for diastolic intervals of 150 ms, 50 ms, and 20 ms respectively. Similarly, normalized atrial currents were 0.96 ± 0.018 , 0.84 ± 0.028 , and 0.72 ± 0.058 for intervals of 150 ms, 50 ms, and 20 ms respectively. Conversely, behavior during trains was different when test pulse duration was fixed at 20 ms (Figure 8, top panels). In the presence of 5 μM AZD1305 steady-state block increased only at the shortest diastolic interval, and this block at 20 ms diastolic interval was greater in atrial myocytes ($p<0.05$). Steady-state currents were 0.72 ± 0.10 and 0.88 ± 0.022 in atrial (top, left panel) vs ventricular myocytes (top, right panel).

Further atrial-ventricular differences of AZD1305-induced inhibition of I_{Na} are shown in Figure 9. In panel A, steady state inactivation using a conditioning step of 100 ms is plotted along the same axis for atrial (filled circles, solid line) and ventricular myocytes (filled triangles, solid line). At resting potentials between -80 mV and -90 mV, there is a greater availability of atrial sodium channels when compared to ventricular sodium channels. Protocols were repeated 4 min after addition of 5 μM AZD1305 (atrial drug open circle, dotted line and ventricular drug open triangle, dotted line). AZD1305 caused a greater hyperpolarizing shift in the atrial inactivation curve when compared to the ventricular curve. These results suggest a lower availability of atrial sodium channels at equivalent potentials. Panel B shows that AZD1305-induced tonic and steady state inhibition of atrial sodium channels is greater when compared to ventricular sodium channels. I_{Na} was recorded during a train of 200 ms pulses with a diastolic interval of 150 ms in control solution and after addition of 5 μM AZD1305. Currents then were normalized to the control current during pulse 1 to reveal both tonic block during the first pulse and steady state block during the 40th pulse. Figure 9B shows a greater tonic and steady-state AZD1305-induced I_{Na} block in atrial cells.

Antiarrhythmic effects of AZD1305 in coronary-perfused right atrial preparations

Acetylcholine (0.5-1.0 μM) dramatically abbreviated atrial APD, permitting very rapid pacing and the induction of AF in 100% of atria ($n=10$). In five atria, we added ACh to the perfusate containing 3 μM AZD1305 and attempted to induce AF with programmed electrical stimulation and rapid pacing. No persistent or sustained AF was induced in any of the five atrial preparations (Table), only brief episodes of atrial flutter or tachycardia (lasting <3 sec) were recorded in 2 atria. Antiarrhythmic action of AZD1305 was associated with a reduction of excitability leading to failure of rapid stimulation to permit 1:1 response (Figure 10A). Atrial APD₉₀ was abbreviated by ACh to a lesser degree in the presence of AZD1305 (3 μM , Table).

In separate series, we first induced persistent AF in the presence of ACh and then tested the ability of AZD1305 to terminate the arrhythmia. Addition of 1 μM AZD1305 terminated persistent AF in 2 out of 6 atria (in 5.0 ± 2.5 min after the start of drug perfusion). Among four atria in which AF persisted after 1 μM AZD1305, an increase of concentration of to 3 μM terminated AF in three. In another series of four atria, the initial tested concentration of 3 μM AZD terminated persistent ACh-mediated AF in all four atria (Figure 10B). Thus, at a concentration of 3 μM , AZD1305 terminated AF in 7 of 8 atria (9.9 ± 7.0 min after the start of 3 μM perfusion). Following AF termination, only non-sustained atrial flutter or fibrillation (<2 min duration) could be induced with programmed electrical stimulation or rapid pacing in 3 out of 7 atria.

DISCUSSION

Our data demonstrate that AZD1305 causes atrial-predominant APD prolongation and atrial-selective depression of sodium channel-dependent parameters, both *in vitro* and *in vivo* in the canine heart, without significantly altering hemodynamic parameters *in vivo*. Consistent with these electrophysiological findings, AZD1305 is shown to produce a much greater inhibition

of I_{Na} in isolated atrial than in ventricular myocytes. Finally, AZD1305 effectively suppresses ACh-mediated AF in *in vitro* models of AF consisting of coronary-perfused right atria.

The use of anti-AF agents is complicated by the risk of induction of severe ventricular arrhythmias. A number of investigational agents developed over the past decade have been shown to produce atrial-selective electrophysiological effects capable of suppressing AF, thus reducing the risk of induction of ventricular proarrhythmia. Atrial selective agents include those that inhibit I_{Kur} , I_{Na} , I_{KACh} and constitutively-active I_{KACh} .^{16; 17} I_{Kr} blockers may also prolong APD and ERP predominantly in atria.^{2; 4; 5}

It is noteworthy that AZD7009 (a congener of AZD1305) was shown to slow conduction and increase DTE in atria, but not in the canine ventricle *in vivo*, consistent with atrial-selective inhibition of I_{Na} .¹¹ Both AZD1305 and AZD7009 primarily block I_{Kr} , I_{Na} , and I_{Ca} , with less pronounced inhibition of I_{Kur} .^{7; 10; 18} The present study demonstrates that AZD1305 depresses sodium channel dependent parameters (V_{max} , conduction time, and DTE) as well as induces PRR in an atrial-predominant manner. The relatively small change in early repolarization with AZD1305 suggests that there is no major reduction in I_{Kur} (Figure 1A). This is consistent with the finding of a much greater IC_{50} for I_{Kur} inhibition by AZD1305 than those of I_{Na} or I_{Kr} .¹⁰ Of note, block of I_{Kur} with 4-aminopyridine (4-AP) or AVE0118 causes significant changes in the upper part of atrial action potential.^{19; 20} Atrial-predominant prolongation of APD by AZD1305 is likely due to block of I_{Kr} . Indeed, at normal heart rates, selective I_{Kr} blockers such as E-4031, dofetilide, ibutilide and almokalant preferentially prolong the atrial vs. ventricular ERP and/or APD.^{2; 4; 5; 21} It is unlikely that block of I_{Kur} by AZD1305 contributes to the atrial preferential APD prolongation, for two reasons: 1) AZD1305 does not appear to inhibit I_{Kur} significantly¹⁰ and, 2) reduction of I_{Kur} abbreviates APD₇₀₋₉₀ in normal (non-remodeled) canine or human atria.^{20; 22} The effect of AZD1305 to prolong atrial APD, and thus eliminate the diastolic interval during which the recovery from the sodium channel largely occurs, likely contributes to the preferential blockade of sodium channel in atria at rapid pacing rates (Figure 2A). Elimination of the diastolic interval leads to greater accumulation of use-dependent block because dissociation of the drug from the channel is impeded.

In contrast to normal pacing rates, at slow pacing rates ventricles, but not atria, display a significant APD prolongation as well as a potential to develop early afterdepolarizations and Torsade de Pointes (TdP) arrhythmias when I_{Kr} is selectively reduced.^{23; 24} This constitutes a major safety drawback of AADs that potently and selectively block I_{Kr} . Although strongly blocking I_{Kr} and prolonging ventricular repolarization, AZD1305 does not induce TdP, neither in a highly sensitive TdP rabbit model¹⁰ nor in the canine LV wedge preparation (Di Diego et al., unpublished). In fact, AZD1305 suppresses dofetilide-induced TdP in rabbit.¹⁰ The low proarrhythmic potential is likely due to the effect of AZD1305 to block the late inward sodium and the L-type calcium currents, thus antagonizing its blockade of I_{Kr} .^{10; 25} These inward currents have been suggested of crucial importance for initiating TdP and seem especially prominent in cells with intrinsically long action potential durations such as the Purkinje fiber and subendocardial ventricular M cells. Similar protective mechanisms have been proposed for other AADs that inhibit I_{Kr} but do not induce TdP (e.g., amiodarone, vernakalant, and ranolazine).

While AZD1305-induced prolongation of ERP in ventricular preparations is due principally to the effect of the drug to prolong of the APD, prolongation of ERP in atrial preparations is due to both prolongation of APD and the development of PRR as a consequence of sodium channel blockade. Of note, although we refer to this as PRR, repolarization is not totally complete at APD₇₅ and the terminal part of phase 3 repolarization no doubt contributes to the depression of excitability and prolongation of PRR. Interestingly, selective I_{Kr} blockers do not

produce PRR despite extension of the terminal part of phase 3.^{5; 21} The atrial-selective effect of AZD1305 to induce PRR is similar to that of ranolazine and chronic amiodarone.^{3; 5}

Major factors contributing to the atrial-selective effects of sodium channel blockers include differences in resting membrane potential (which is more depolarized in atrial vs. ventricular cells) and biophysical properties of sodium channels of atrial vs. ventricular myocytes (see ^{9; 26} for review). The half-inactivation voltage ($V_{0.5}$) of canine atrial myocytes is 12 to 16 mV more negative than that of ventricular myocytes.^{3; 27}

There appears to be a difference in ranolazine vs. AZD1305 atrial selective block of I_{Na} . While block of ranolazine is principally due to use-dependent inhibition of I_{Na} ,²⁸ atrial selective inhibition of I_{Na} by AZD1305 is due to tonic blockade as well (Figure 9). Under control conditions, atrial myocytes are slower to recover from inactivation at -90 mV, and both dynamic and steady-state inactivation curves are more negative than those of ventricular cells. Addition of AZD1305 slowed this recovery and shifted these curves further to the left, reducing availability of sodium channels. However, there is also a crucial contribution of use-dependent block of I_{Na} in atrial selectivity of AZD1305 at rapid activation rates due to the loss of diastolic interval in atria, but not ventricles (Figure 2A).

AZD1305 is very effective in suppressing and preventing the induction of AF in the ACh-mediated AF model (see Table). Anti-AF effects of AZD1305 are likely due to its ability to prolong APD and to depress excitability, leading to the development of PRR. Block of I_{Kur} has been shown to prolong atrial repolarization in electrically remodeled atria (i.e., having a tri-angular shape action potential) and may contribute to AZD1305-induced APD prolongation in atria in the presence of ACh^{20; 22}. Of note, the clinical efficacy of the AZD1305 analogue AZD7009 to acutely convert AF is high and comparable to that of electrical cardioversion (82% vs. 83%, respectively).¹⁴

Limitations of the study

The atrial selectivity of AZD1305 was determined acutely in healthy hearts *in vitro* and *in vivo*. The anti-AF efficacy of AZD1305 was also determined in “healthy” atria exposed to ACh. Clinical cardiac arrhythmias are normally associated with electrical and structural abnormalities, which may significantly modulate pharmacological responses, anti-arrhythmic efficacy, and safety.

Acknowledgments

We gratefully acknowledge the expert technical assistance of Judy Hefferon and Robert Goodrow.

Disclosure of Funding: Supported by a grant from AstraZeneca R&D Mölndal, Sweden, grant HL47678 from NHLBI (CA) and the Free and Accepted Masons of New York State and Florida

REFERENCES

1. Yue L, Feng J, Li GR, Nattel S. Characterization of an ultrarapid delayed rectifier potassium channel involved in canine atrial repolarization. *J Physiol* 1996;496(Pt 3):647–62. [PubMed: 8930833]
2. Spinelli W, Parsons RW, Colatsky TJ. Effects of WAY-123,398, a new class III antiarrhythmic agent, on cardiac refractoriness and ventricular fibrillation threshold in anesthetized dogs: a comparison with UK-68798, E-4031, and dl-sotalol. *J Cardiovasc Pharmacol* 1992;20(6):913–22. [PubMed: 1282594]
3. Burashnikov A, Di Diego JM, Zygmunt AC, Belardinelli L, Antzelevitch C. Atrium-selective sodium channel block as a strategy for suppression of atrial fibrillation: differences in sodium channel inactivation between atria and ventricles and the role of ranolazine. *Circulation* 2007;116(13):1449–57. [PubMed: 17785620]

4. Baskin EP, Lynch JJ Jr. Differential atrial versus ventricular activities of class III potassium channel blockers. *J Pharmacol Exp Ther* 1998;285(1):135–42. [PubMed: 9536003]
5. Burashnikov A, Di Diego JM, Sicouri S, Ferreiro M, Carlsson L, Antzelevitch C. Atrial-selective effects of chronic amiodarone in the management of atrial fibrillation. *Heart Rhythm* 2008;5(12):1735–42. [PubMed: 19084813]
6. Fedida D. Vernakalant (RSD1235): a novel, atrial-selective antifibrillatory agent. *Expert Opin Investig Drugs* 2007;16(4):519–32.
7. Persson F, Carlsson L, Duker G, Jacobson I. Blocking characteristics of hKv1.5 and hKv4.3/hKChIP2.2 after administration of the novel antiarrhythmic compound AZD7009. *J Cardiovasc Pharmacol* 2005;46(1):7–17. [PubMed: 15965349]
8. Gogelein H, Brendel J, Steinmeyer K, Strubing C, Picard N, Rampe D, Kopp K, Busch AE, Bleich M. Effects of the atrial antiarrhythmic drug AVE0118 on cardiac ion channels. *Naunyn Schmiedeberg Arch Pharmacol* 2004;370(3):183–92. [PubMed: 15340774]
9. Burashnikov A, Antzelevitch C. Atrial-selective sodium channel block for the treatment of atrial fibrillation. *Expert Opin Emerg Drugs* 2009;14(2):233–49. [PubMed: 19466903]
10. Carlsson L, Andersson B, Linhardt G, Lofberg L. Assessment of the ion channel-blocking profile of the novel combined ion channel blocker AZD1305 and its proarrhythmic potential versus dofetilide in the methoxamine-sensitized rabbit in vivo. *J Cardiovasc Pharmacol* 2009;54(1):82–9. [PubMed: 19528812]
11. Goldstein RN, Khrestian C, Carlsson L, Waldo AL. Azd7009: a new antiarrhythmic drug with predominant effects on the atria effectively terminates and prevents reinduction of atrial fibrillation and flutter in the sterile pericarditis model. *J Cardiovasc Electrophysiol* 2004;15(12):1444–50. [PubMed: 15610294]
12. Lofberg L, Jacobson I, Carlsson L. Electrophysiological and antiarrhythmic effects of the novel antiarrhythmic agent AZD7009: a comparison with azimilide and AVE0118 in the acutely dilated right atrium of the rabbit in vitro. *Europace* 2006;8(7):549–57. [PubMed: 16798770]
13. Crijns HJ, Van G, I, Walfridsson H, Kulakowski P, Ronaszeki A, Dedek V, Malm A, Almgren O. Safe and effective conversion of persistent atrial fibrillation to sinus rhythm by intravenous AZD7009. *Heart Rhythm* 2006;3(11):1321–31. [PubMed: 17074639]
14. Geller JC, Egstrup K, Kulakowski P, Rosenqvist M, Jansson MA, Berggren A, Edvardsson N, Sager P, Crijns HJ. Rapid conversion of persistent atrial fibrillation to sinus rhythm by intravenous AZD7009. *J Clin Pharmacol* 2009;49(3):312–22. [PubMed: 19129422]
15. Carlsson L, Chartier D, Nattel S. Characterization of the in vivo and in vitro electrophysiological effects of the novel antiarrhythmic agent AZD7009 in atrial and ventricular tissue of the dog. *J Cardiovasc Pharmacol* 2006;47(1):123–32. [PubMed: 16424796]
16. Nattel S, Carlsson L. Innovative approaches to anti-arrhythmic drug therapy. *Nat Rev Drug Discov* 2006;5(12):1034–49. [PubMed: 17139288]
17. Burashnikov A, Antzelevitch C. New pharmacological strategies for the treatment of atrial fibrillation. *Ann Noninvasive Electrocardiol* 2009;14(3):290–300. [PubMed: 19614642]
18. Persson F, Carlsson L, Duker G, Jacobson I. Blocking characteristics of hNav1.5, and hKvLQT1/hminK after administration of the novel antiarrhythmic compound AZD1309. *J Cardiovasc Electrophysiol* 2005;16(3):329–41. [PubMed: 15817095]
19. Burashnikov A, Mannava S, Antzelevitch C. Transmembrane action potential heterogeneity in the canine isolated arterially-perfused atrium: effect of I_{K_r} and $I_{to}/I_{K_{ur}}$ block. *Am J Physiol* 2004;286:H2393–H2400.
20. Wettwer E, Hala O, Christ T, Heubach JF, Dobrev D, Knaut M, Varro A, Ravens U. Role of $I_{K_{ur}}$ in controlling action potential shape and contractility in the human atrium: influence of chronic atrial fibrillation. *Circulation* 2004;110(16):2299–306. [PubMed: 15477405]
21. Wiesfeld AC, De Langen CD, Crijns HJ, Bel KJ, Hillege HL, Wesseling H, Lie KI. Rate-dependent effects of the class III antiarrhythmic drug almokalant on refractoriness in the pig. *J Cardiovasc Pharmacol* 1996;27(4):594–600. [PubMed: 8847879]
22. Burashnikov A, Antzelevitch C. Can inhibition of $I_{K_{ur}}$ promote atrial fibrillation? *Heart Rhythm* 2008;5(5):1304–9. [PubMed: 18774108]

23. Antzelevitch C, Shimizu W, Yan GX, Sicouri S, Weissenburger J, Nesterenko VV, Burashnikov A, Di Diego JM, Saffitz J, Thomas GP. The M cell: its contribution to the ECG and to normal and abnormal electrical function of the heart. *J Cardiovasc Electrophysiol* 1999;10(8):1124–52. [PubMed: 10466495]
24. Burashnikov A, Antzelevitch C. Late-phase 3 EAD. A unique mechanism contributing to initiation of atrial fibrillation. *PACE* 2006;29(3):290–5. [PubMed: 16606397]
25. Andersson B, Abi-Gerges N, Carlsson L. The combined ion channel blocker AZD1305 attenuates late Na current and IKr-induced action potential prolongation and repolarization instability. *Europace*. 2010 In press.
26. Burashnikov A, Antzelevitch C. Atrial-selective sodium channel blockers: do they exist? *J Cardiovasc Pharmacol* 2008;52(2):121–8. [PubMed: 18670368]
27. Li GR, Lau CP, Shrier A. Heterogeneity of sodium current in atrial vs epicardial ventricular myocytes of adult guinea pig hearts. *J Mol Cell Cardiol* 2002;34(9):1185–94. [PubMed: 12392892]
28. Zygmunt AC, Nesterenko VV, Rajamani S, Hu D, Barajas-Martínez H, Belardinelli L, Antzelevitch C. Mechanism of the preferential block of the atrial sodium current by ranolazine. *Biophys J* 2009;96:250a. Abstract.

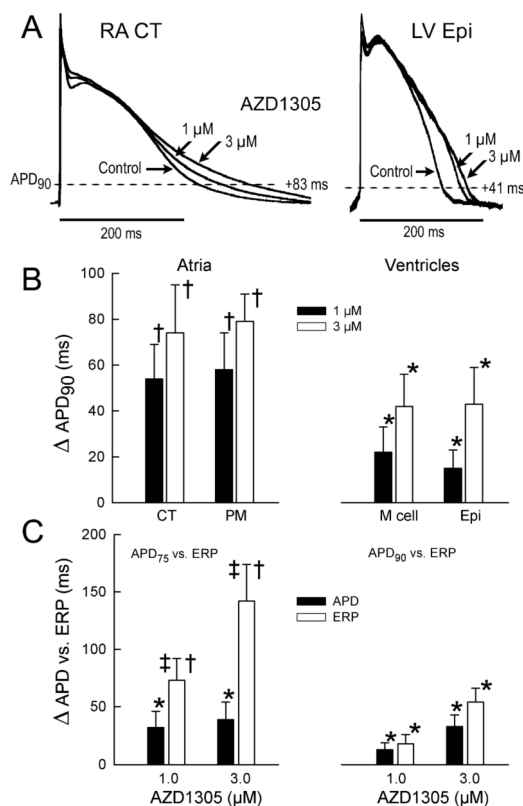
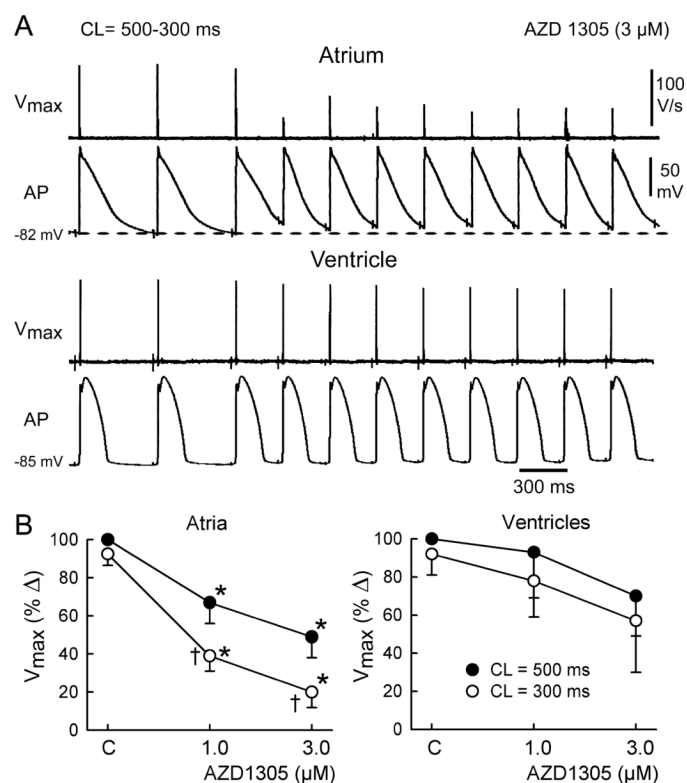


Figure 1.

AZD1305 induces atrial-selective post-repolarization refractoriness (PRR). **A:** Superimposed action potential recorded from right atrial crista terminalis (RA CT) and left ventricular epicardium (LV Epi). Dashed lines denote the level of APD₉₀ and the numbers indicate the changes in APD₉₀ induced by 3 μM AZD1305. **B:** Change in action potential duration at 90% repolarization (APD₉₀) in atria and ventricles induced by AZD1305. CT – crista terminalis; PM – pectinate muscle; M cell – M cell region; Epi – epicardium. **C:** Induction of PRR in atrial but not ventricular preparations. PRR is approximated as the differences between ERP and APD₇₅ in atria and APD₉₀ in ventricles. Note that atrial ERP coincides with action potential duration at 75% repolarization (APD₇₅), whereas ventricular ERP generally coincides with APD₉₀. “Atria” - data were obtained from PM region. “Ventricles” - ERP was recorded from endocardial surface and APD from immediate subendocardium (about 2 mm from the surfaces). * - $p < 0.05$ vs. control; † - $p < 0.001$ vs. control; ‡ - $p < 0.05$ vs. respective APD₇₅. CL = 500 ms. n=8-12.

**Figure 2.**

AZD1305 produces a greater use-dependent reduction of maximum rate of rise of the AP upstroke (V_{max}) in atrial vs. ventricular preparations.

A: Transmembrane action potentials and respective V_{max} values recorded upon shortening of cycle length (CL) from 500 to 300 ms. **B:** Summary data of the effects of AZD1305 on V_{max} in atrial and ventricular preparations. All data are normalized to control V_{max} value recorded at a CL of 500 ms. Atrial and ventricular data were obtained from the crista terminalis and the M cell region, respectively. *- $p < 0.05$ vs. respective controls (C), † - $p < 0.05$ vs. CL 500 ms. $n = 7-14$.

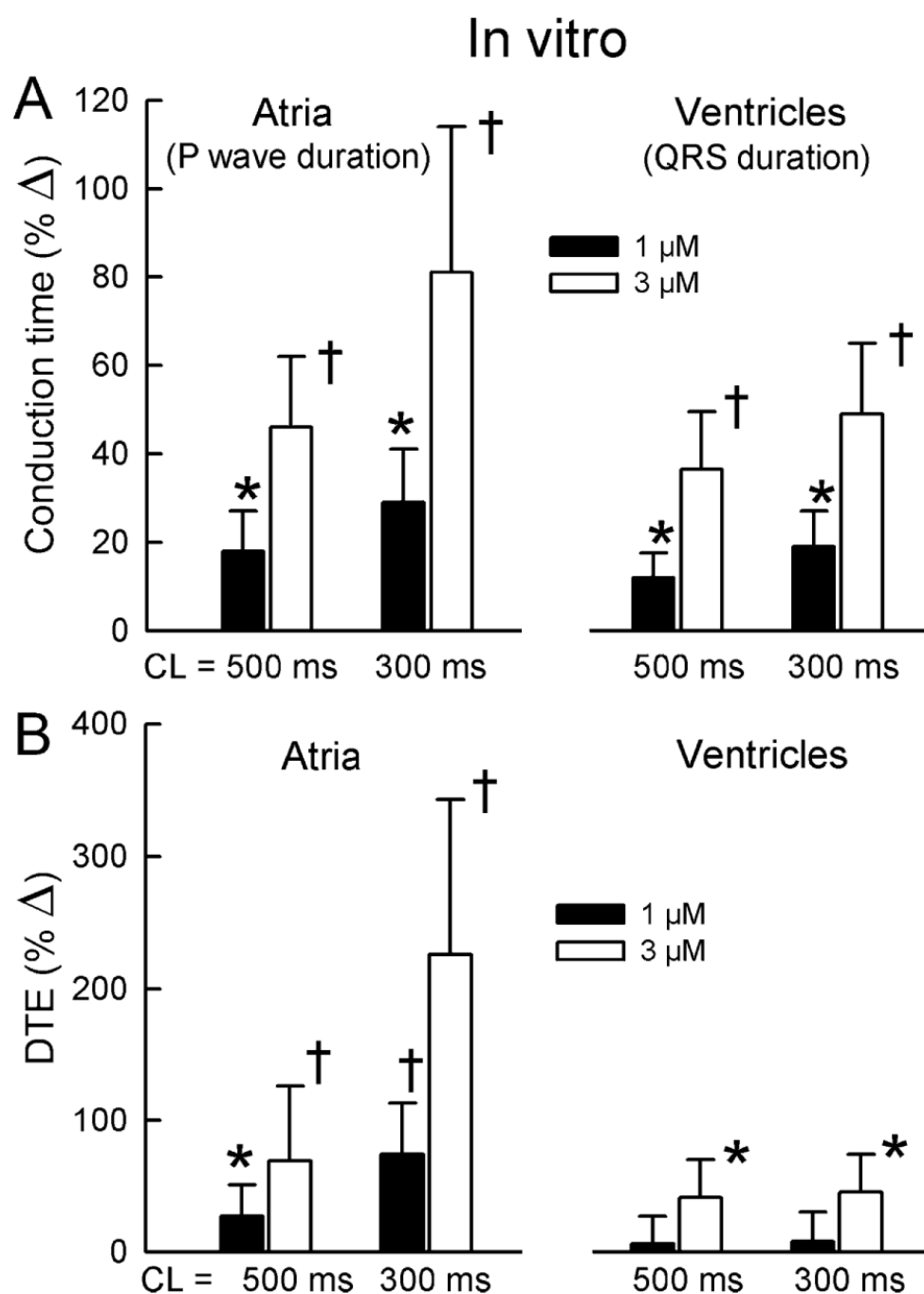
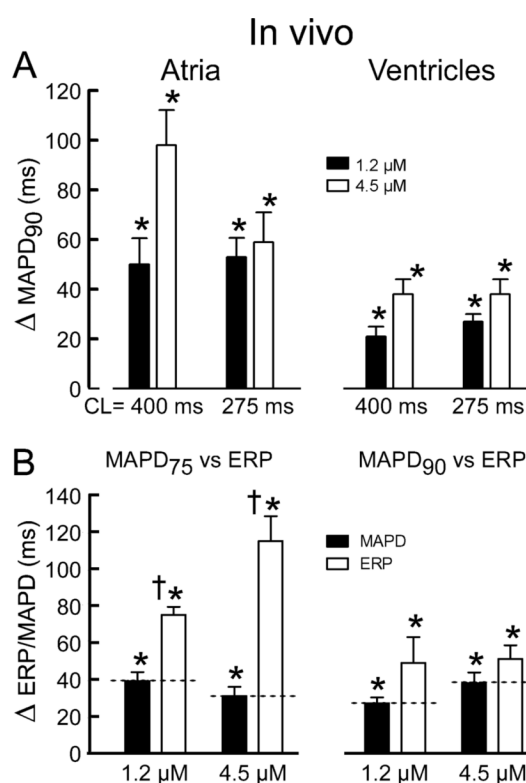
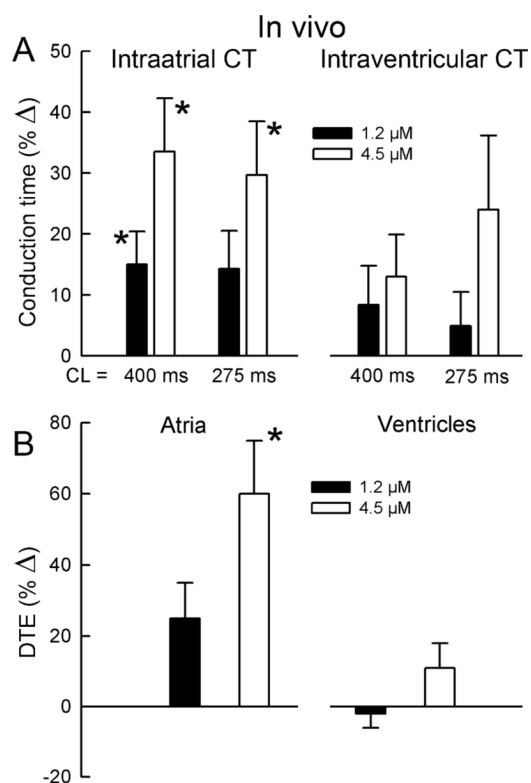


Figure 3.

AZD1305 causes a greater increase in conduction time (A) and diastolic threshold of excitation (DTE, B) in atrial vs. ventricular coronary-perfused preparations. * - $p < 0.05$ vs. respective controls; † - $p < 0.001$ vs. respective controls. Cycle length (CL) = 500 ms. $n = 5-20$.

**Figure 4.**

AZD1305 produces a greater prolongation of repolarization and effective refractory period (ERP) in canine atrium vs. ventricle *in vivo*. Post-repolarization refractoriness (PRR) develops primarily in the atrium. **A:** AZD1305 prolongs monophasic action potential duration (MAPD₉₀) more in atria vs. ventricles. **B:** Atrial-selective development of PRR (cycle length (CL) = 275 ms). Note that atrial MAPD was assessed at 75% repolarization. Data were obtained from the endocardial surface of right atrium and right ventricle. Effects were assessed at pseudo steady-state plasma concentrations of 1.2 and 4.5 μM (n=8). * p<0.05 vs. respective control; † p<0.001 vs MAPD₇₅.

**Figure 5.**

Preferential effects of AZD1305 to increase conduction time and depress excitability in atria vs. ventricles. * $P < 0.05$ vs. control ($n=8$). The diastolic threshold of excitation (DTE) data were measured at a cycle length (CL) of 275 ms.

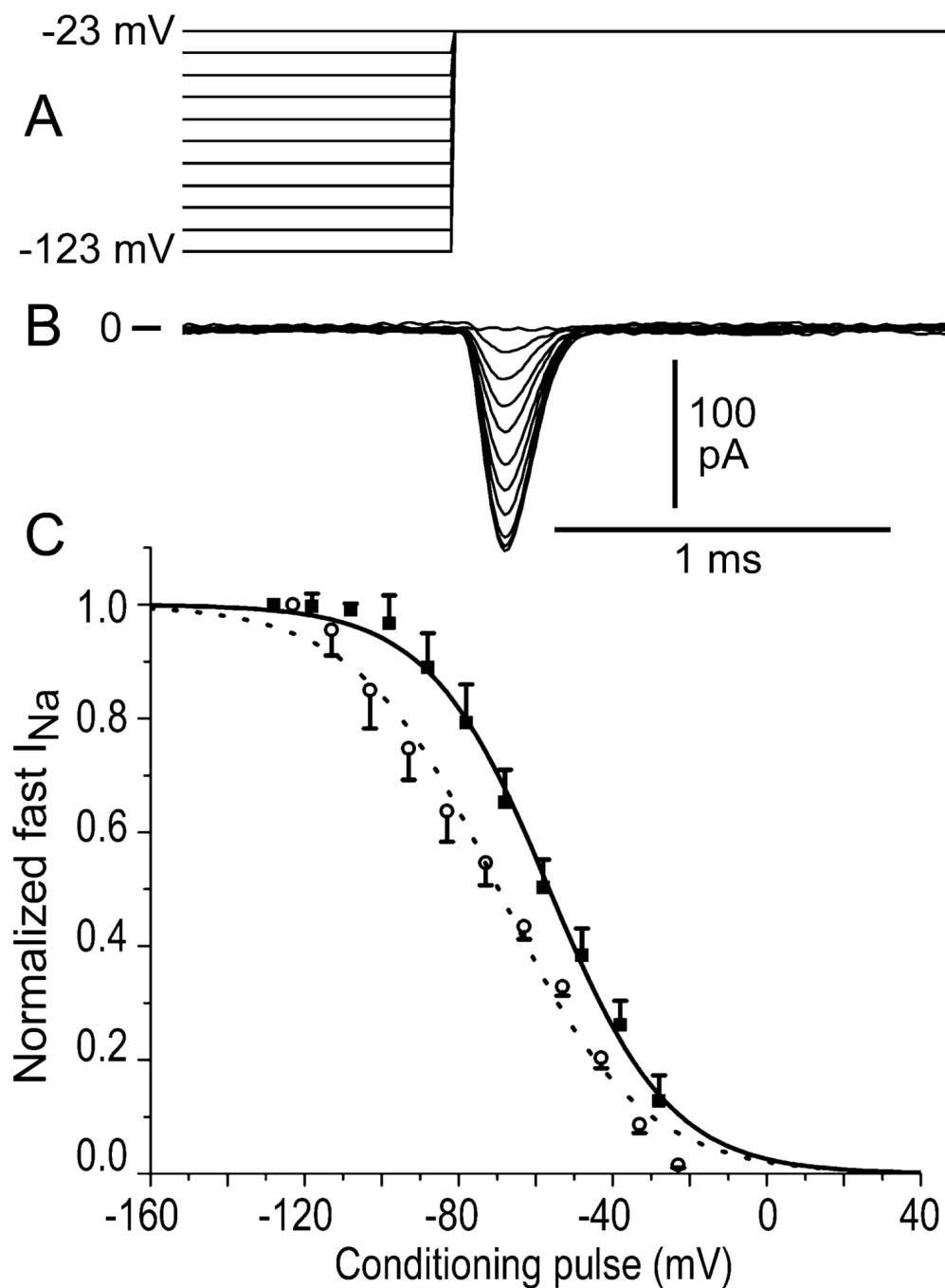


Figure 6.

Comparison of steady state inactivation curves in atrial and ventricular myocytes from normal adult dogs. Voltage protocol (A), fast I_{Na} (B), and steady state inactivation curves (C) from right atrial (mean \pm S.E.M., open circles) and left ventricular myocytes (filled squares). Half-inactivation for atrial myocytes showed a significant negative shift compared to ventricular myocytes ($p < 0.05$, $n = 3$).

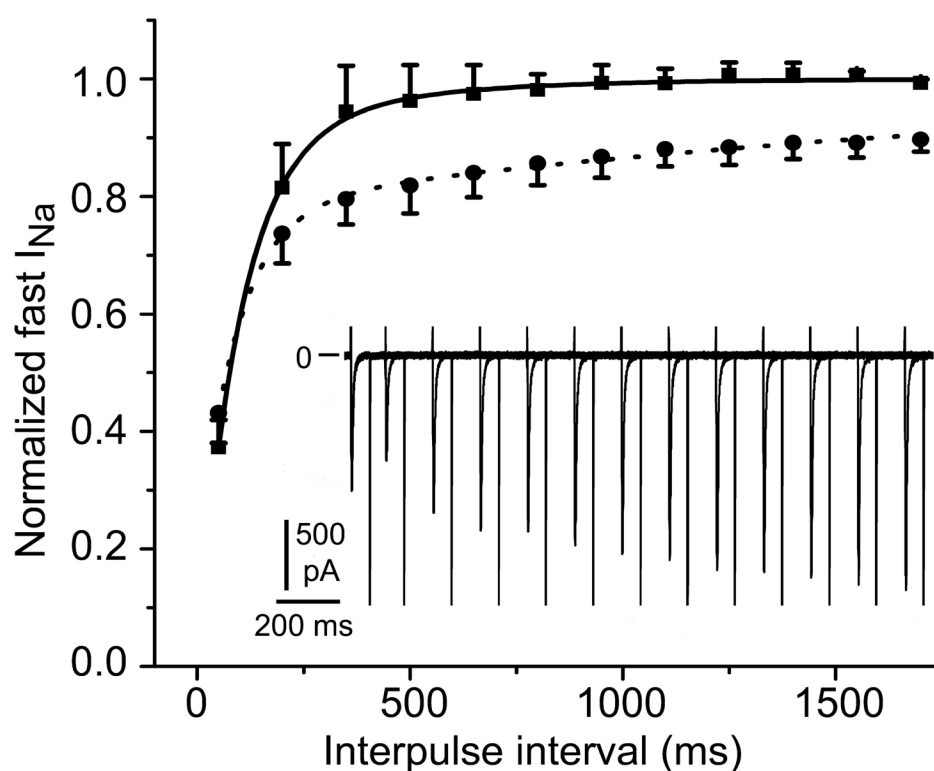


Figure 7.

Recovery of fast I_{Na} following a rapid train of 40 pulses in drug-free solutions. Holding potential -90 mV. Biexponential fit for recovery of 5 right atrial myocytes (dotted line) and 6 left ventricular endocardial myocytes (solid line). Mean \pm S.E.M. The insert shows partial recovery of fast I_{Na} in a representative right atrial myocyte (vertical calibration pA, horizontal calibration seconds).

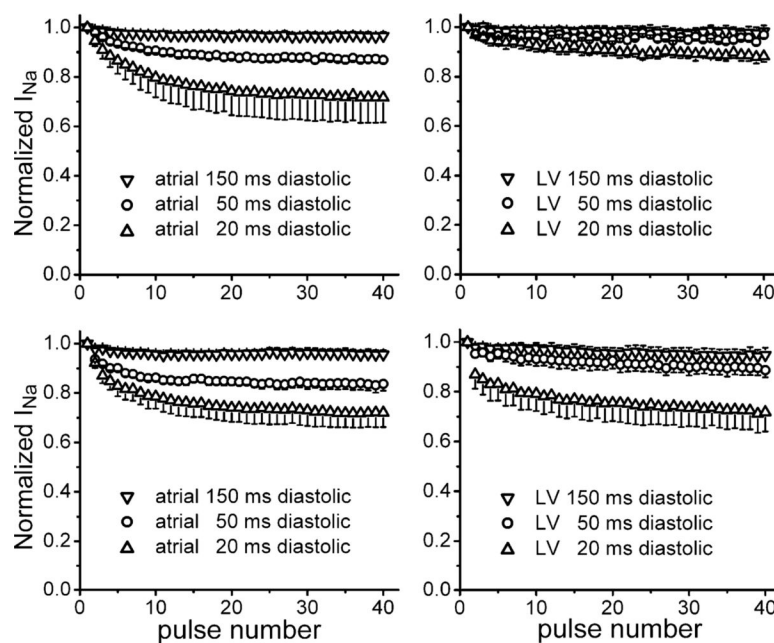


Figure 8.

Dependence of AZD1305-induced use-dependent block of I_{Na} on diastolic interval in atrial (left panels, 3–7 myocytes) and ventricular myocytes (right panels, 2–5 myocytes). Test pulse duration was 20 ms in top panels and 200 ms in bottom panels. Holding potential = -140 mV. Shown are mean \pm SEM.

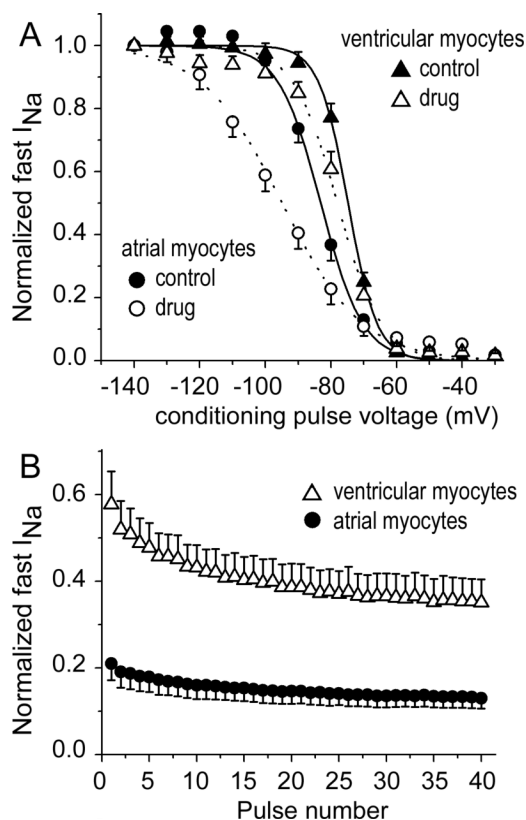


Figure 9.

Effects of 5 μM AZD1305 on I_{Na} in canine atrial (circles, n=8 cells) and ventricular myocytes (triangles, n = 8 cells). **A:** Immediately following a train of 40 pulses the drug caused a hyperpolarizing shift in steady state inactivation curves, and this shift was greater for atrial myocytes. I_{Na} was recorded in control solution and 4 min after addition of 5 μM AZD1305.

B: Tonic block and steady-state block of I_{Na} following trains of pulses were greatest in atrial myocytes. I_{Na} was recorded in control solution and 4 min after addition of 5 μM AZD1305 in atrial myocytes (n=5 cells) and ventricular myocytes (n=7).

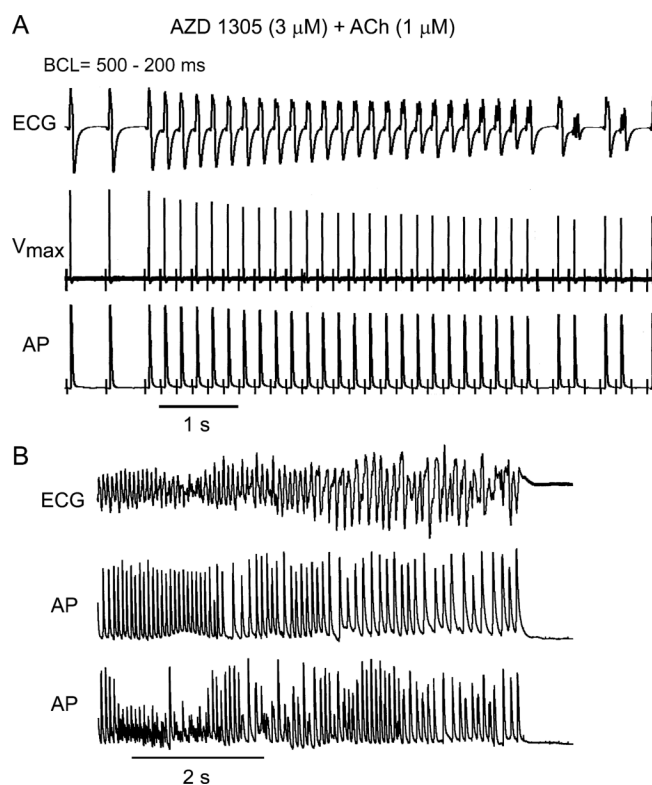


Figure 10.

AZD1305 terminates persistent atrial fibrillation (AF) and prevents induction of AF in an acetylcholine-mediated model of AF. **A:** AZD1305 prevents induction of AF by reducing excitability and preventing 1:1 activation at a basic cycle length (BCL) of 200 ms. V_{max} trace show use-dependent depression sodium channel activity. **B:** Termination of persistent acetylcholine-mediated AF by AZD1305 (3 μ M) in a coronary-perfused atrial preparation. Shown are simultaneously recorded ECG and two action potential traces at the moment of AF termination. AP=Action potential

Table

Effects of AZD1305 (3 μ M) to suppress atrial excitability and ACh-mediated AF in the isolated canine coronary perfused right atria.

	APD ₉₀ (ms)	ERP (ms)	Shortest S ₁ -S ₁	Persistent AF Induction	Persistent AF Termination	Prevention of Persistent AF re-induction
Control	205 \pm 8	145 \pm 13	126 \pm 7	0%	-	-
AZD1305	283 \pm 17 [*]	287 \pm 46 [*]	310 \pm 46 [*]	0%	-	-
ACh	43 \pm 7	46 \pm 5	54 \pm 5	100% (10/10)	0% (0/10)	-
ACh + AZD1305	91 \pm 12 [†]	110 \pm 35 [†]	166 \pm 36 [†]	0% (0/5)	88% (7/8)	100% (7/7)

Experiments to prevent atrial fibrillation (AF) induction and terminate AF were performed in different atria. Action potential duration (APD) and effective refractory period (ERP) data presented in the table were obtained from the pectinate muscle region of coronary-perfused atria at a cycle length (CL) of 500 ms (n=5-10).

ACh – acetylcholine (1.0 μ M). Shortest S₁-S₁ – the shortest CL permitting 1:1 activation (at a diastolic threshold of excitability \times 2 determined at a CL of 500 ms).

^{*} <0.05 vs. control
[†] P<0.05 vs. ACh alone.